Size-dependent internalization of particles via the pathways of clathrin- and caveolae-mediated endocytosis

Joanna REJMAN, Volker OBERLE, Inge S. ZUHORN and Dick HOEKSTRA[1]

Department of Membrane Cell Biology, University of Groningen, A. Deusinglaan 1, 9713 AV Groningen, The Netherlands

Non-phagocytic eukaryotic cells can internalize particles < 1 μm in size, encompassing pathogens, liposomes for drug delivery or lipoplexes applied in gene delivery. In the present study, we have investigated the effect of particle size on the pathway of entry and subsequent intracellular fate in non-phagocytic B16 cells, using a range of fluorescent latex beads of defined sizes (50–1000 nm). Our data reveal that particles as large as 500 nm were internalized by cells via an energy-dependent process. With an increase in size (50–500 nm), cholesterol depletion increased the efficiency of inhibition of uptake. The processing of the smaller particles was significantly perturbed upon microtubule disruption, while displaying a negligible effect on that of the 500 nm beads. Inhibitor and co-localization studies revealed that the mechanism by which the beads were internalized, and their subsequent intracellular routing, was strongly dependent on particle size. Internalization of microspheres with a diameter < 200 nm involved clathrin-coated pits. With increasing size, a shift to a mechanism that relied on caveolae-mediated internalization became apparent, which became the predominant pathway of entry for particles of 500 nm in size. At these conditions, delivery to the lysosomes was no longer apparent. The data indicate that the size itself of (ligand-devoid) particles can determine the pathway of entry. The clathrin-mediated pathway of endocytosis shows an upper size limit for internalization of approx. 200 nm, and kinetic parameters may determine the almost exclusive internalization of such particles along this pathway rather than via caveolae.

Key words: caveolae, endocytosis, gene delivery, microsphere uptake, particle size.

INTRODUCTION

In recent years, cationic-lipid-mediated gene transfer has become a versatile tool for cellular transfection, relevant to fundamental cell biological research and gene therapy alike (reviewed in [1,2]). However, the interaction between DNA and cationic lipids is difficult to control, resulting in the formation of complexes ('lipoplexes') that display a very heterogeneous size distribution. Often, the particle size ranges from 100 nm to > 1 μm, and, evidently, the efficiency of cellular uptake and subsequent intracellular processing, a prerequisite for effective cellular transfection, may well depend on particle size. Although the molecular details of the mechanism by which cationic lipid carriers mediate DNA delivery are still poorly understood, current evidence supports the hypothesis that the cationic lipid–DNA complexes enter cells by means of endocytosis. Subsequently, a 'perturbation' of the endosomal membrane occurs, causing release of the complex-associated plasmid into the cytosol, eventually leading towards nuclear integration of the gene [3–8]. Yet, a number of different endocytic pathways can be distinguished, utilized by eukaryotic cells to internalize a large variety of substances, and which might affect the kinetics of intracellular complex processing and thereby transfection efficiency itself. These pathways include phagocytosis, macropinocytosis, clathrin-mediated endocytosis and non-clathrin-mediated endocytosis, the latter including internalization via caveolae. It is believed that such a diverse range of mechanisms is used by cells to accomplish different tasks.

In previous work, we demonstrated that cationic lipid–DNA complexes primarily transfect cells, following complex internalization via the pathway of clathrin-mediated endocytosis [9]. However, in this previous work, it could not be excluded that a minor fraction entered cells via caveolae. Caveolae are invaginated, flask-shaped plasma membrane domains, which are especially enriched in cholesterol and sphingolipids. They are characterized by the presence of the integral membrane protein caveolin. Interestingly, caveolae can internalize large molecular complexes, such as cholera toxin [10], and may serve as a portal of entry for certain viruses such as SV40 (simian virus 40) [11,12] and bacteria [13]. In fact, in this manner, bacteria (or viruses) might escape delivery to and digestion in lysosomes [13]. Analogously, by avoiding lysosomal targeting, as occurs along the pathway of receptor-mediated endocytosis, such a pathway could thus be advantageous in carrier-mediated drug and DNA delivery. Moreover, another previous study [8] hinted that size might be an important parameter in the pathway of particle entry. The purpose of the present study was therefore to investigate the effect of particle size on the pathway of entry and processing by cells. However, since it is virtually impossible to produce homogeneous populations of lipoplexes of well-defined sizes, we systematically studied the uptake of fluorescent latex particles of defined sizes by non-phagocytic mouse melanoma B16 cells. In this manner, insight was obtained into the size-dependent regulation of particle internalization via an endocytic mechanism.

MATERIALS AND METHODS

Cell culture

The murine melanoma cell line B16-F10 was cultured in Dulbecco's modified Eagle's medium containing 10 % (v/v)

Abbreviations used: AP, adaptor protein; BODIPY®, 4,4-difluoro-4-bora-3a,4a-diaza-*s*-indacene; diIC$_{18}$, 1,1′-dioctadecyl-3,3,3′,3′-tetramethylindocarbocyanine perchlorate; DOPE, dioleoylphosphatidylethanolamine; Eps15, epidermal growth factor receptor pathway substrate clone 15; GFP, green fluorescent protein; HBSS, Hanks balanced salt solution; LacCer, lactosylceramide; MβCD, methyl-β-cyclodextrin; SAINT2, *N*-methyl-4(dioleyl)methylpyridinium chloride; SV40, simian virus 40.

[1] To whom correspondence should be addressed (e-mail d.hoekstra@med.rug.nl).

© 2004 Biochemical Society

foetal calf serum and 100 μg/ml penicillin/streptomycin (Gibco BRL, Life Technology, Merelbeke, Begium) with 5 % CO_2 at 37 °C.

Fluorescent microspheres

Fluorescent microspheres Fluoresbrite® YG (yellow–green; λ_{ex}, 445 nm; λ_{em}, 500 nm) and Fluoresbrite® YO (yellow–orange; λ_{ex}, 535 nm; λ_{em}, 570 nm) were purchased from Polysciences (Warrington, PA, U.S.A.). Their sizes were 50, 100, 200, 500 and 1000 nm in diameter.

The microspheres were incubated with B16 cells in serum-free medium. Removal of attached beads was accomplished by washing the cells three times (10 min) with 0.2 M ethanoic acid/0.5 M NaCl. In addition, cells were washed with a 0.4 % (w/v) Trypan Blue solution [9,14] to quench extracellular fluorescence, thus enabling determination of the fraction that was actually internalized.

FACS analysis

A Coulter Elite flow cytometer was used to perform FACS analysis. After incubation with microspheres, the cells were washed three times and detached by trypsinization. After centrifugation, the cells were resuspended in a 0.4 % (w/v) Trypan Blue solution in Hanks balanced salt solution (HBSS) to quench the extracellular fluorescence. The treated samples were subsequently washed twice, and analysed by flow cytometry, with 5000–10 000 cells measured in each sample.

Cholesterol depletion

Cholesterol depletion was carried out essentially as described previously [9], with 10 mM methyl-β-cyclodextrin (MβCD) [15–17], in the presence of 1 μg/ml lovastatin (Sigma) for 1 h at 37 °C.

Cytoskeletal disruption

The cells were pre-incubated with 10 μg/ml nocodazole (Sigma) for 60 min at 37 °C to disrupt microtubuli. Consecutively, microspheres of 50, 100, 200 or 500 nm in diameter were added and incubated in serum-free cell-culture medium in the presence of the drug.

Potassium depletion

B16 cells were washed once with potassium-free buffer, pH 7.4, containing 140 mM NaCl, 20 mM Hepes, 1 mM $CaCl_2$, 1 mM $MgCl_2$, 1 mg/ml D-glucose, followed by a wash with hypotonic buffer (potassium-free buffer diluted with water, 1:1). Then, the cells were washed again three times with potassium-free buffer. Control cells were treated with buffer, pH 7.4, containing 140 mM NaCl, 20 mM Hepes, 1 mM $CaCl_2$, 1 mM $MgCl_2$, 1 mg/ml D-glucose and 10 mM KCl. Microspheres of different sizes were incubated with the cells in potassium-free or potassium-containing buffer, as indicated. Subsequently, the cells were analysed by FACS.

Treatment with other drugs/inhibitors

B16 cells were treated with genistein (200 μM) [18,19], filipin (5 μg/ml) [20,21], chlorpromazine (10 μg/ml) [22] or 5-(*N*,*N*-dimethyl)amiloride hydrochloride (10 μM) [23] (all from Sigma), in serum-free culture medium for 1 h, at 37 °C. Subsequently, fluorescent latex beads were added and the incubation was continued for another 2 h, after which the cells were analysed by FACS.

Expression of Eps15 (epidermal growth factor receptor pathway substrate clone 15) mutants

In the present study, we employed two GFP (green fluorescent protein)–Eps15 constructs (gifts from Dr Alexandre Benmerah and Dr Alice Dautry-Varsat, Pasteur Institute, Paris, France), Eps15 (DIII), and a mutant form deprived of AP-2 (adaptor protein-2)-binding sites (D3Δ2). B16 cells were transfected with the GFP–DIII and GFP–D3Δ2 constructs using SAINT2 (*N*-methyl-4(dioleyl) methylpyridinium chloride)/DOPE (dioleoylphosphatidylethanolamine) as the carrier system, as previously described [9]. At 2 days after transfection, the cells were incubated with differently sized beads in serum-free medium for 3 h at 37 °C. After intense washing, cells were treated with Trypan Blue, washed three times in HBSS and examined by confocal microscopy (Leica TCS SP2; Germany): λ_{ex}, 488 nm and λ_{em}, 530 nm for GFP; λ_{ex}, 535 nm and λ_{em}, 570 nm for red beads.

Co-localization of beads with BODIPY® (4,4-difluoro-4-bora-3a,4a-diaza-*s*-indacene)–LacCer (lactosylceramide) or caveolin

For BODIPY®–LacCer co-localization studies, cells were incubated with the lipid analogue (1 μM) in the presence of fluorescent microspheres for 30 min at 10 °C. The lag time between adding the beads and the lipid was 5 min. After 90 min of incubation at 37 °C, the medium was removed and the cells were washed once in HBSS after which they were treated with Trypan Blue, as described above, and analysed by confocal microscopy (Leica TCS SP2).

For co-localization of the beads with caveolin, the B16 cells were washed three times with serum-free medium and then were incubated with fluorescent latex beads for 30 min at 4 °C to promote their interaction with the plasma membrane. To trigger internalization, the cells were subsequently incubated at 37 °C for 30 min, after which time interval they were fixed for 30 min in 4 % (w/v) paraformaldehyde. The cells were permeabilized with 0.2 % (v/v) Triton X-100 and non-specific sites were blocked with PBS containing 1 % (w/v) BSA and 0.2 % (v/v) Triton X-100. Subsequently, the cells were incubated with the primary antibody against caveolin 1 (rabbit pAb; Transduction Laboratories Pharmingen, Alphen a/d Rijn, The Netherlands) diluted 1:100, for 16 h at 4 °C. After washing with PBS, the primary antibody was coupled with FITC-labelled anti-rabbit IgG antibody at a dilution of 1:75 for 45 min at room temperature (20 °C). For microscopy, the cells were embedded in mounting medium from DAKO (Carpinteria, CA, U.S.A.). The cells were examined by confocal scanning microscopy as above.

Lysosome staining

LysoTracker Red

B16 cells were first incubated with fluorescent microspheres (green) for 2 h (37 °C, serum-free medium). After extensive washing, the lysosomal marker, LysoTracker Red (Molecular Probes, Eugene, OR, U.S.A.), was applied (50 pM at 37 °C for 1 h). Subsequently, the cells were washed and treated with extracellular quencher [0.4 % (w/v) Trypan Blue].

© 2004 Biochemical Society

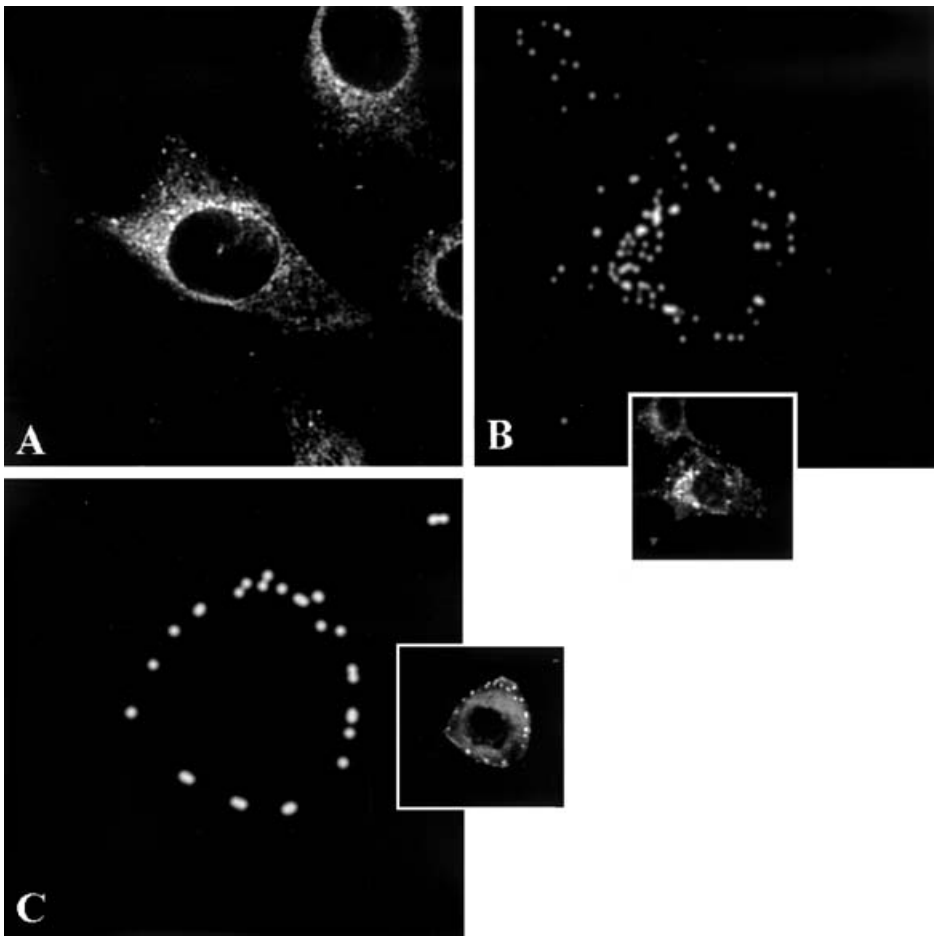

Figure 1 Size-dependent internalization of fluorescently labelled microspheres

The cells were incubated at 37 °C with fluorescently labelled microspheres of 50 (for 1 h) (**A**), 200 (3 h) (**B**) or 500 (3 h) (**C**) nm in diameter and then washed three times for 10 min with 0.2 M ethanoic acid/0.5 M NaCl solution to remove surface-bound beads. Alternatively, to ascertain visualization of the internalized fraction only, the cells were treated with the fluorescence-quenching dye Trypan Blue (0.4 %), as described in the Materials and methods section. The samples were subsequently examined by confocal microscopy (Leica TCS SP2). The insets represent corresponding phase-contrast images.

FITC–dextran

Alternatively, B16 cells were first incubated with FITC–dextran (green) for 12 h at 37 °C to allow the dye to accumulate in the endo/lysosomal compartments. The cells were incubated with fluorescent microspheres (red) in serum-free medium for 4 h at 37 °C. After washing and quenching the cell-associated particles, samples were studied by means of confocal microscopy (Leica TCS SP2).

RESULTS

Efficiency of uptake of beads is dependent on size

To determine the effect of particle size on the pathway of internalization by non-phagocytic cells, fluorescently labelled microspheres of 50, 100, 200, 500 and 1000 nm in diameter were incubated with mouse melanoma B16 cells. Evidence of uptake was obtained by confocal microscopy and FACS. To discriminate between cell-association and actual internalization, extracellular fluorescence was quenched by addition of Trypan Blue, the non-quenched fraction thus representing internalized beads [14]. The data revealed that the cells took up particles up to a size of 500 nm at 37 °C (Figure 1), i.e. no uptake was seen of particles 1 μm in size. From quantitative data obtained by FACS, we estimate that, relative to internalized 50 nm beads, the uptake of the 100 nm beads was diminished by approx. 3–4-fold, whereas the internalization of the 200 and 500 nm beads was reduced by approx. 8–10 times. Internalization of beads with diameters of 50 and 100 nm started immediately at 37 °C after initial binding at 4 °C (Figure 2), and continued for approx. 3 h. Over a time interval of 30 min, some 50 % of the cell-associated beads were internalized, as determined by Trypan Blue quenching (see above). In contrast, little, if any, uptake of 500 nm beads was seen over a period of 30 min, and significant accumulation within the cells could be only detected after 2–3 h.

Examination of the cells by fluorescence microscopy revealed further that the internalized beads of 50, 100 and 200 nm were distributed throughout the cells (Figures 1A, 1B and 2). Following a subsequent chase, the particles accumulated in the perinuclear region of the cells. In contrast, 500 nm beads were localized largely at the periphery of the cells (Figure 1C), irrespective of the incubation time or that of the subsequent chase (results not shown; cf. Figure 1C). No internalization of the beads was seen at 4 °C.

© 2004 Biochemical Society

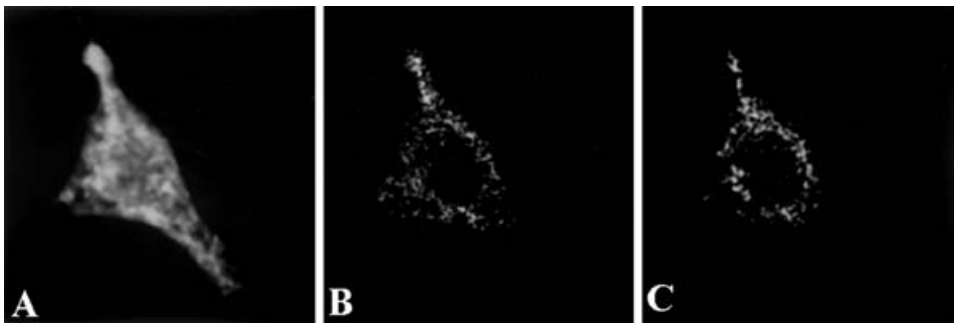

Figure 2 Internalization of fluorescently labelled 50 nm microspheres

Microspheres of 50 nm were first incubated with the cells at 4 °C, to allow binding (30 min). The unbound beads were removed by extensively washing the cells with ice-cold HBSS buffer (five times). Internalization, following warming up, was examined by confocal microscopy (Leica TCS SP2). Pictures were obtained at different time points: 0 (**A**), 5 (**B**) and 20 (**C**) min. Diffuse cell-surface staining was gradually replaced with a distinct intracellular localization of the beads, which eventually accumulated near the perinuclear region of the cell.

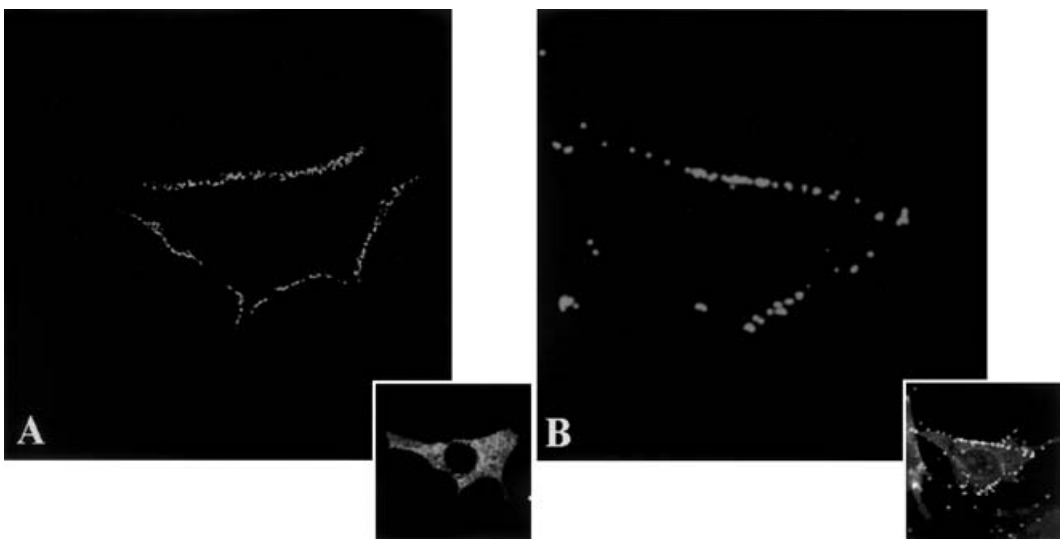

Figure 3 Microtubule disruption perturbs the intracellular processing of internalized beads

The cells were incubated with nocodazole (10 μg/ml) for 60 min at 37 °C, before addition of the beads. Subsequently, microspheres were added to the solution and incubated for 2 h at 37 °C. The cells were then acid-washed and/or treated with Trypan Blue to remove and/or quench extracellular fluorescence respectively. The samples were examined by confocal microscope (Leica TCS SP2). Note that incubation of the cells with nocodazole caused the accumulation of 50 (**A**) and 200 (**B**) nm particles just beneath the plasma membrane.

Microtubule disruption affects particle internalization and processing in a size-dependent manner

Although quantitative differences in particle internalization were observed (see above), those with a diameter up to 200 nm were relatively rapidly processed, and accumulated in the perinuclear region of the cell (see Figure 1B; cf. Figure 2 for 50 nm beads). This process was microtubule-dependent. Thus pre-incubation of the cells with nocodazole caused the accumulation of 50, 100 and 200 nm particles near the plasma membrane (Figure 3). Presumably, disruption of the microtubules precluded intracellular trafficking of these beads from early to late endosomes. A quantitative analysis of the internalized fractions by FACS following this treatment revealed further that, apart from intracellular processing, the effective internalization was also modulated. The amount of internalized 50 and 100 nm microspheres was reduced by $> 50\,\%$ in nocodazole-treated cells. Interestingly, the uptake of 200 nm beads was diminished by only 25 %, whereas both the internalization and intracellular distribution of the 500 nm particles remained unchanged. Accordingly, these data suggest that, in a size-dependent manner, differences exist in the potential control and mechanism of internalization, a point of inflection becoming apparent at a size of approx. 200 nm.

Internalization of the beads is diminished by cholesterol depletion

In recent years, it has been well-established that different types of endocytosis can operate simultaneously and that some of those are susceptible to cholesterol depletion [9,15–17,24,25]. It was therefore of interest to examine whether size-dependent distinctions in internalization could be revealed as a function of cholesterol depletion. To this end, the cells were pre-treated with MβCD and were incubated in the presence of lovastatin, an inhibitor of *de novo* synthesis of cholesterol [9,17]. As shown in Figure 4, the internalization of the beads was affected by cholesterol depletion, showing a tendency towards decreased internalization

© 2004 Biochemical Society

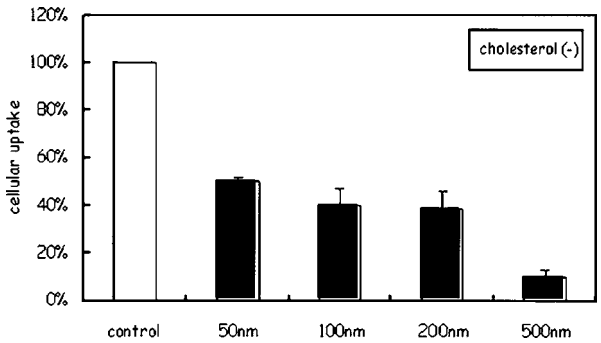

Figure 4 Differential effect of cholesterol depletion on the internalization of microspheres

The cells were pre-incubated with 10 mM MβCD for 1 h at 37 °C. Lovastatin (1 μg/mg) was present during both cholesterol depletion and the subsequent incubation. Beads of 50, 100, 200 or 500 nm were added and the cells were incubated for 2 h at 37 °C. Evidence of uptake was obtained by FACS. The fluorescence intensity of beads in control cells was set at 100 %. Irrespective of size, the uptake of the microspheres was reduced, suggesting that efficient internalization requires cholesterol. However, uptake of the 500 nm microspheres was affected most prominently. For each size of microsphere, three independent experiments were carried out in duplicate.

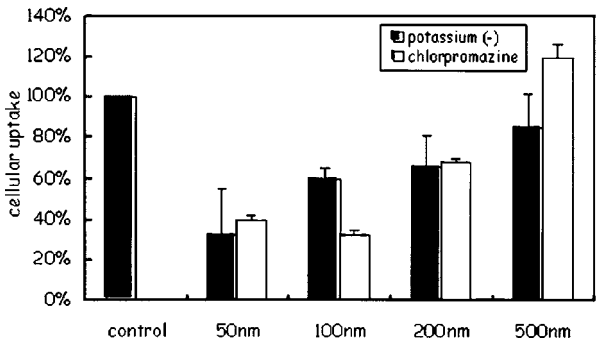

Figure 5 Effect of inhibitors of clathrin-mediated endocytosis on the internalization of microspheres

B16 cells were first washed with potassium-free buffer, pH 7.4, consisting of 140 mM NaCl, 20 mM Hepes, 1 mM $CaCl_2$, 1 mM $MgCl_2$ and 1 mg/ml D-glucose. It was followed by rinsing with hypotonic buffer (potassium-free buffer diluted with water, 1:1). The cells were then washed again three times with potassium-free buffer. Control cells were treated with buffer, pH 7.4, composed of 140 mM NaCl, 20 mM Hepes, 1 mM $CaCl_2$, 1 mM $MgCl_2$, 1 mg/ml D-glucose and 10 mM KCl. Microspheres of different sizes were incubated with the cells in potassium-free or potassium-containing buffer for 60 min at 37 °C. Alternatively, B16 cells were pre-treated with chlorpromazine (10 μg/ml) in serum-free cell-culture medium for 1 h, at 37 °C. After this period, fluorescent latex beads were added and incubated for 2 h. For each size of microsphere, three separate experiments were carried out in duplicate.

with increased particle size, the uptake of the 500 nm particles becoming inhibited by >90 %. Both caveolae- [20,21,26–28] and clathrin-mediated endocytosis [9,17,29] have been shown to depend on cholesterol. However, recent evidence also suggests a role for cholesterol in macropinocytosis [25], although such a mechanism is likely to be of less relevance in non-professional endocytosing cells, such as B16 cells. Yet, interestingly, the data in Figure 4 reveal different susceptibilities, in particular when comparing the 200 nm beads with the 500 nm beads, implying distinct cholesterol-dependent internalization mechanisms. To discriminate further between these mechanisms, the following experiments were carried out.

The mechanism of bead internalization is size-dependent; clathrin versus caveolin coats

Transferrin is generally accepted as a ligand exclusively internalized via the clathrin-coated-pit pathway. Therefore we employed FITC–transferrin as a model compound to adjust concentrations of inhibitors utilized for blocking this pathway of endocytosis. Internalization of fluorescent microspheres was studied at concentrations, which entirely inhibited the uptake of transferrin.

Previously, we have shown that depletion of intracellular potassium inhibits clathrin-mediated endocytosis of a (heterogeneous) mixture of lipoplexes (mean diameter of approx. 200 nm) [9]. To examine whether or not the ensuing inhibition of transfection efficiency, as observed, resulted from an inhibition of the internalization of a defined population, we next examined the extent to which microsphere uptake was inhibited as a function of size. We adopted a procedure in which cells were first subjected to hypotonic shock and then transferred to isotonic potassium-free buffer, resulting in rapid depletion of cellular potassium [30]. Figure 5 shows that, in potassium-depleted cells, the uptake of microspheres decreases with decreasing diameter, the 50 nm beads showing the highest degree of inhibition (approx. 70 %), whereas internalization of the 500 nm beads was barely affected (15 %).

A similar pattern of inhibition as a function of diameter was observed for microsphere uptake by cells pre-treated with chlorpromazine, which perturbs clathrin-processing and thereby clathrin-mediated endocytosis [22]. In this case, the inhibition of internalization of microspheres with sizes between 200 and 50 nm progressively decreased from 70 to 30 %, whereas the uptake of those with a diameter of 500 nm was unaltered or even slightly higher (Figure 5).

To obtain further support for the observations that apparently the smaller beads are preferentially internalized via the pathway of clathrin-mediated endocytosis, we overexpressed dominant-negative constructs of Eps15, which have been shown to inhibit clathrin-dependent endocytosis [31,32]. In the present study, we employed two Eps15 constructs generated by Benmerah et al. [31] in which GFP was fused to the entire C-terminal domain of Eps15 (DIII overexpression of which highly inhibited transferrin endocytosis) or a mutant form (D3Δ2) deprived of all AP-2 binding sites (overexpression of which did not change uptake of transferrin). Thus B16 cells were transfected with GFP–DIII and GFP–D3Δ2 constructs using SAINT2/DOPE as a plasmid carrier system, as described previously [9]. The cells were subsequently incubated with the fluorescent microspheres. Overexpression of the entire C-terminal domain (DIII) inhibited the internalization of 200 nm beads (Figure 6B). The lack of AP-2-binding sites in the construct restored the internalization of 200 nm particles (Figure 6D). These data are consistent with the inhibition observed upon chlorpromazine treatment (Figure 5), suggesting a dependence of clathrin-coat mediated uptake. In contrast, as shown in Figures 6(A) and 6(C), the internalization of the 500 nm particles was equally effective in the cells transfected with two different constructs and non-transfected cells, implying that their entry into the cell is insensitive to the changes in the organization of the clathrin-coated pits.

Since B16 cells are non-phagocytic cells, a significant contribution of macropinocytosis to the internalization of the large beads at non-stimulating conditions, was considered less likely. Indeed, several pieces of evidence argued against such a contribution. When cells had been pre-treated with the macropinocytosis inhibitor 5-(*N*,*N*-dimethyl)amiloride hydrochloride (see the Materials and methods section) or cytochalasin D, the level of internalization of the 500 nm beads was essentially indistinguishable from that observed for non-treated cells, determined

© 2004 Biochemical Society

© 2004 Biochemical Society

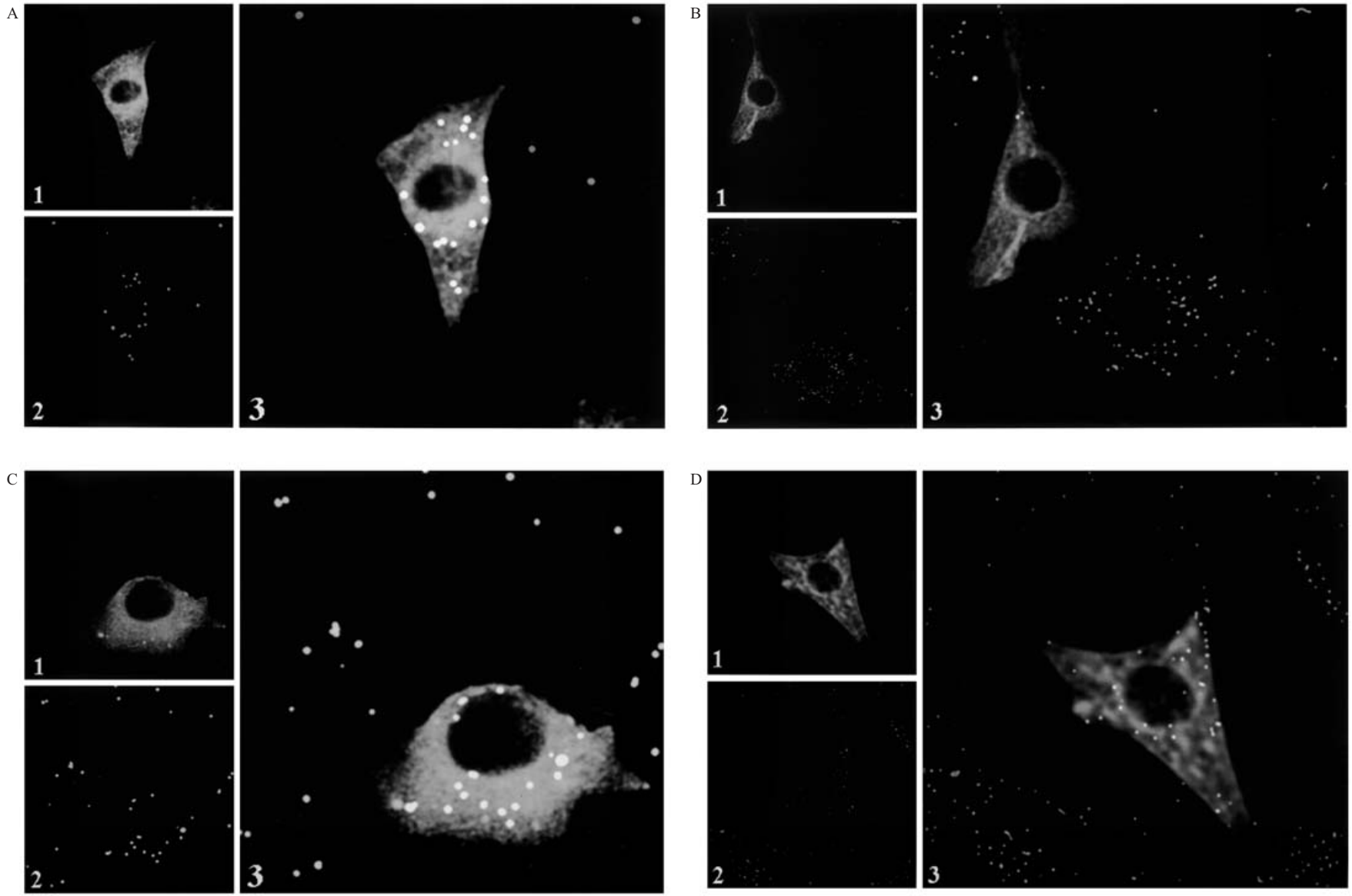

Figure 6 Effect of expression of a dominant negative Eps15 mutant, interfering with clathrin-mediated endocytosis, on the internalization of the beads

B16 cells were transfected with GFP–DIII [(**A**) and (**B**); endocytosis mutant] or GFP-D3Δ2 [(**C**) and (**D**); control] constructs, using the SAINT2/DOPE carrier system. Lipoplexes were made by mixing DNA and SAINT liposomes (molar charge ratio, 1:2.5). B16 cells were plated on coverslips 1 day before transfection. Complexes were incubated with the cells for 4 h at 37 °C. After this period, the cells were washed and treated with serum-containing medium, which was refreshed after 24 h of cultivation. At 2 days after transfection, the cells were incubated with 200 (**B**) and (**D**) or 500 (**A**) and (**C**) nm beads in serum-free medium for 3 h at 37 °C. After extensive washing, the cells were rinsed with Trypan Blue, washed three times in HBSS and examined by confocal microscopy (Leica TCS SP2): λ_{ex}, 488 nm and λ_{em}, 530 nm for GFP; λ_{ex}, 535 nm and λ_{em}, 570 nm for red beads. (**A**) Panel 1, DIII-positive cells; panel 2, 500 nm beads; panel 3, merged picture. (**B**) Panel 1, DIII-positive cells; panel 2, 200 nm beads; panel 3, merged picture. (**C**) Panel 1, D3Δ2-positive cells; panel 2, 500 nm beads; panel 3, merged picture. (**D**) Panel 1, D3Δ2-positive cells; panel 2, 200 nm beads; panel 3, merged picture.

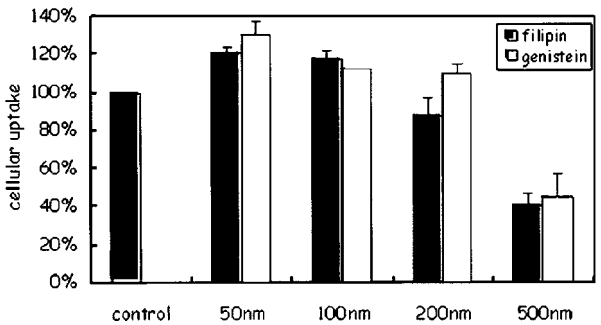

Figure 7 Effect of inhibitors of caveolae-mediated endocytosis on microsphere uptake

Filipin (5 μg/ml), a sterol-binding agent that selectively inhibits caveolae invagination without affecting the function of coated pits, or genistein (200 μM) were incubated with the cells for 1 h, at 37 °C. Subsequently, fluorescent latex beads were added and incubated for the subsequent 2 h in the presence of inhibitors. Evidence of uptake was obtained by FACS. The fluorescence intensity of beads in control cells was set as 100 %. Note that the inhibitors only affected the internalization of the 500 nm beads, i.e. leaving internalization of $\leqslant$200 nm microspheres unaltered. Results are means $\pm$ S.D. from three independent experiments, carried out in duplicate.

as described above. Moreover, following addition of 500 nm beads, membrane ruffling of diIC$_{18}$ (1,1′-dioctadecyl-3,3,3′,3′-tetramethylindocarbocyanine perchlorate)-labelled plasma membranes was never observed (results not shown; see Discussion). Therefore, we next investigated whether or not these larger particles could be internalized along the pathway of caveolae-mediated endocytosis.

The sphingolipid LacCer is internalized almost exclusively via a caveolae-mediated pathway [9,33]. This lipid marker was therefore employed to verify the effectiveness of a variety of potential inhibitors of this pathway in B16 cells, caveolae being also present at the surface of these cells [34]. Thus inhibitors, as indicated below, used at concentrations that completely inhibited the internalization of BODIPY®-labelled LacCer, were subsequently employed to examine the ability of such an inhibitor to block internalization of the beads as well.

Filipin has been reported to specifically block caveolae-mediated uptake [20,21]. When B16 cells had been treated with this compound (1 mg/ml) for 60 min before incubation with microspheres of different sizes, no significant effect was observed on the uptake of the beads with a diameter $\leqslant$100 nm (Figure 7). However, while the uptake of the 200 nm beads was reduced by approx. 20 %, the uptake of the 500 nm particles was reduced by more than 50 %.

Genistein inhibits caveolae-mediated uptake of SV40 [35]. Pre-treatment of the B16 cells with this drug at a concentration that completely inhibited the uptake of BODIPY®–LacCer reduced the uptake of 500 nm microspheres by more than 50 %, whereas the internalization of particles $<$200 nm was relatively unaffected or even slightly enhanced (Figure 7). In line with this observation, as shown in Figure 8(A), a high degree of co-localization of internalized BODIPY®–LacCer and the 500 nm beads was observed, which is consistent with the notion that internalization of the 500 nm microspheres occurs via a caveolae-mediated mechanism. In contrast, as shown in Figure 8(B), there was hardly any co-localization observed for internalized BODIPY®–LacCer and the 200 nm beads, emphasizing the size-dependent differences in the mechanism of uptake.

Further support for a caveolae-mediated pathway of entry of the large 500 nm beads was obtained when investigating the potential co-localization of caveolin, using FITC-labelled antibodies, and the fluorescent 500 nm spheres. The merged confocal micrographs reveal yellow dots, which indicate co-localization of labelled caveolin and the 500 nm beads (Figure 9). No significant co-localization for the smaller beads was seen (results not shown), the appearance being fully in line with the distinct localization of LacCer and the 200 nm beads, as seen in Figure 8(B). Taken together, these data fully agree with the notion that caveolae are prominently and preferentially involved in the internalization of larger latex particles, i.e. with diameters exceeding 200 nm, but less than 1 μm. Hence these data are consistent with a size-dependent internalization of beads via clathrin- and caveolae-mediated pathways.

Beads of 200 nm, but not of 500 nm, arrive in late endosomal/lysosomal compartments

As well as a distinction in the mechanism of internalization, the fate of the particles also appears to be size-dependent, the data suggesting that the smaller beads are able to reach late endosomal/lysosomal compartments after incubation for 4 h at 37 °C. To verify this experimentally, B16 cells were first incubated with FITC–dextran (Figure 10) for 12 h, which was followed by an incubation with fluorescent microspheres for 4 h. Co-localization was observed for dextran and microspheres $\leqslant$200 nm (Figure 10B), but not for 500 nm beads (Figure 10A). These results were confirmed by employing LysoTracker Red (results not shown).

DISCUSSION

Given the heterogeneity of cationic lipid–DNA complexes, it has been difficult to define precisely the effect of lipoplex size on transfection and at what level(s) in the overall transfection process size might be relevant. This prompted us to investigate the internalization of fluorescent latex particles of defined size by a non-phagocytic cell line, the B16 melanoma. In the present study, we have shown that particle size as such can strongly affect the efficiency of cellular uptake, the mode of endocytosis and the subsequent efficiency of particle processing along the endocytic pathway. This insight is of relevance in the context of both fundamental work, e.g. that aimed at defining internalization pathways of micro-organisms, and applied studies, such as in carrier-mediated delivery of drugs. Previous studies demonstrated that epithelial cells can internalize microspheres of $<$100 nm in diameter [36,37]. In the present paper, we demonstrate that microspheres as large as 500 nm are also internalized by non-phagocytic cells. Microspheres with diameters less than 200 nm, and approx. 80 % of the 200 nm beads as such, are internalized via clathrin-coated pits. The 500 nm beads enter the cells by a clathrin-independent pathway, the lower size limit of this pathway becoming gradually apparent at approx. 200 nm, whereas the upper limit is below 1 μm, as these particles are not internalized by the non-phagocytic B16 cells. Internalization of the 500 nm microspheres, but not that of the smaller ones (Figure 7), was prominently inhibited by pre-treatment of the cells with filipin and genistein, both interfering with caveolae-mediated endocytosis [20,22,35], whereas the 500 nm beads, and not the smaller ones, co-localized with the caveolae marker LacCer [33] (Figure 8). Moreover, the data revealing a co-localization of the 500 nm beads and caveolin fully support these observations (Figure 9). In contrast, chlorpromazine, potassium depletion and overexpression of dominant-negative constructs of Eps15 did not affect internalization of the 500 nm beads, but progressively inhibited uptake of particles $\leqslant$200 nm. Accordingly, the data strongly suggest that larger particles (at least 200 nm, but less than

© 2004 Biochemical Society

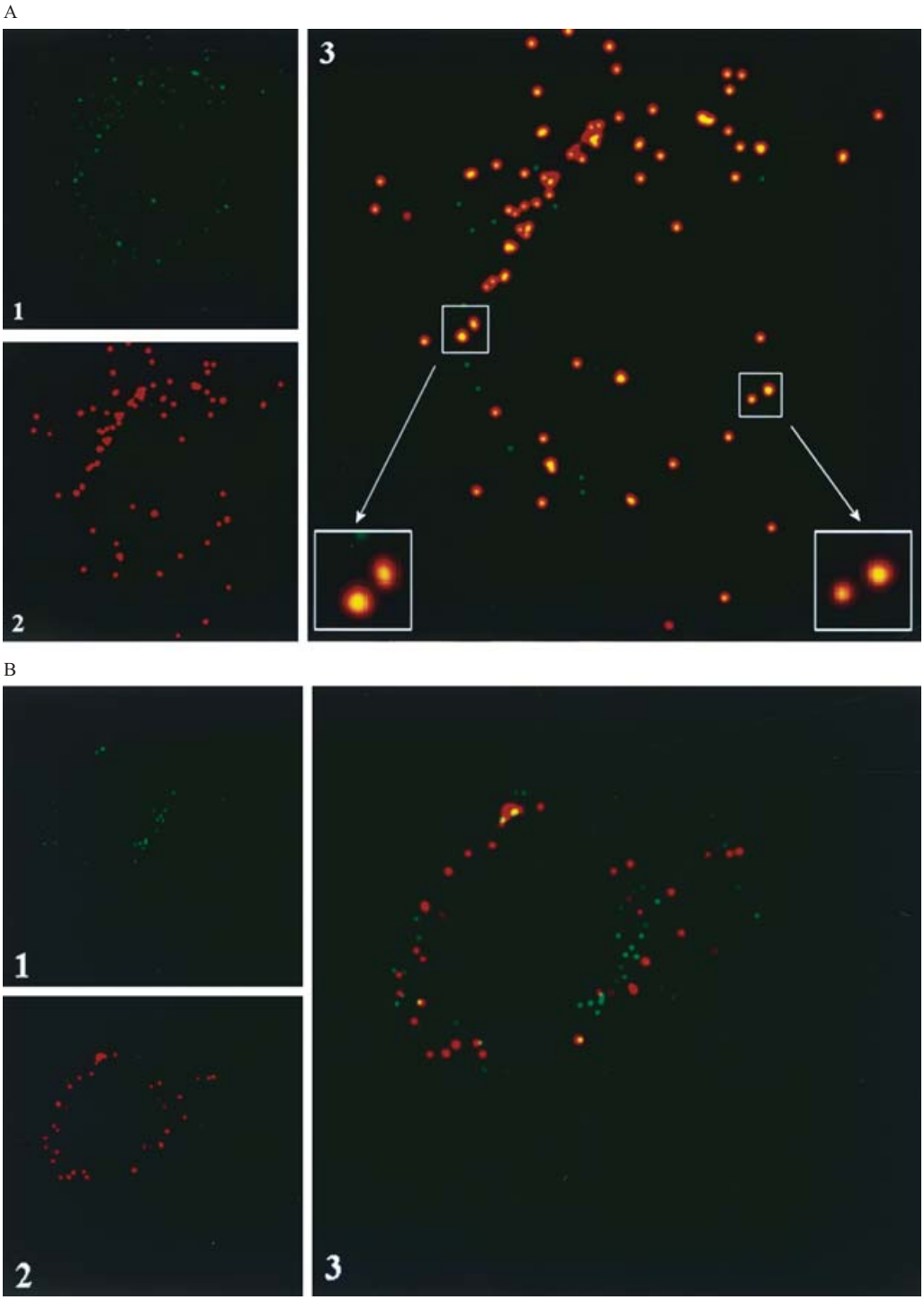

Figure 8 Selective co-localization of internalized BODIPY®–LacCer and microspheres of distinct size

Cells were incubated with BODIPY®–LacCer (1 μM) in the presence of fluorescent microspheres for 30 min at 10 °C. The lag time between adding the beads and the lipid was 5 min. A 90 min incubation at 37 °C was followed by removal of medium and washing in HBSS. After treatment with Trypan Blue, the cells were examined by confocal microscopy (Leica TCS SP2). The merged picture revealed numerous yellow dots indicating the co-localization of the internalized 500 nm beads and LacCer (**A**). In contrast, such a co-localization was not apparent for BODIPY®–LacCer and the 200 nm beads (**B**). (**A**) Panel 1, BODIPY®–LacCer (green); panel 2, 500 nm beads (red); panel 3, merged picture. (**B**) Panel 1, BODIPY®–LacCer (green); panel 2, 200 nm beads (red); panel 3, merged picture.

1 μm in diameter) enter cells preferentially along the pathway of caveolae-mediated endocytosis. Those with a diameter of 200 nm or less are processed along the pathway of clathrin-mediated endocytosis, entirely consistent with previous results that lipoplexes with an mean size of 200 nm are primarily internalized along the same pathway [9].

Internalization of particles with diameters of 50 and 100 nm is a relatively rapid process, showing kinetics reminiscent of

© 2004 Biochemical Society

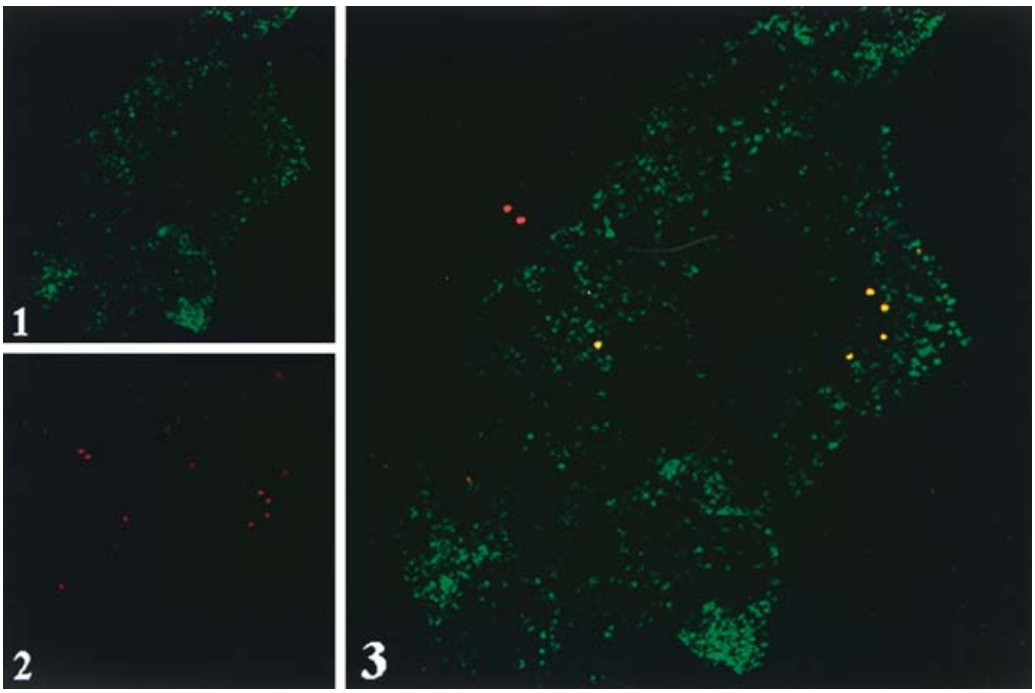

Figure 9 Internalized 500 nm beads co-localize with caveolin-1

B16 cells were incubated with 500 nm diameter fluorescent latex beads for 30 min at 4 °C, which was followed by internalization for 30 min at 37 °C. Caveolae were stained with an antibody against caveolin-1, as described in the Materials and methods section. Panel 1 reveals the localization of caveolin (green), panel 2 that of the beads (red). The merged image is shown in panel 3. Note that the beads localized near the cell periphery are red, whereas those that are in the process of internalization are yellow, reflecting a co-localization of internalized beads and caveolin. See the text for further details.

receptor-mediated internalization of ligands, such as transferrin via coated vesicles. Thus half of the cell-associated fraction of 50–100 nm beads was internalized within 30 min (Figure 2). In contrast, even though 200 nm beads were shown to be internalized via a clathrin-mediated mechanism, their cellular processing was substantially slower, significant internalization becoming apparent only after several hours. Similar (low) rates of cellular processing have been demonstrated earlier for clathrin-mediated uptake of lipoplexes with an mean diameter of 200 nm [9]. Such a size-dependent delay of uptake has also been reported for viral particles [38] and polyplexes [39].

Since our data demonstrate that efficient uptake of microspheres requires cholesterol, we cannot entirely exclude the possibility that macropinocytosis is, to some extent, involved in the internalization of larger particles (>200 nm). This mode of particle internalization, although not ubiquitous, may operate in cells other than macrophages and, as reported recently, is also dependent on the presence of cholesterol in the plasma membrane [25]. However, in light of the specificity of the applied inhibitors and given the co-localization studies, our data at best suggest a minor contribution of such a pathway in the present system. Moreover, it is well established that macropinocytosis requires a functional actin cytoskeleton [25,40–42], whereas the internalization of the 500 nm beads is insensitive to cytochalasin D (results not shown), which is known to block macropinocytosis [43]. Moreover, membrane ruffling, representing a prerequisite for formation of macropinosomes [25], was never observed under these conditions, as visualized by labelling the plasma membrane with the fluorescent lipid dye diIC_{18} (results not shown).

Interestingly, even after 4 h at 37 °C, the larger particles, in contrast with those with diameters of $\leqslant 200$ nm, had not (yet) reached the lysosomal compartment. In fact, these observations may also shed some light on the question why larger lipoplexes might give rise to higher transfection efficiency [8,9,44–46]. Although the net internalization might be less, as compared with the smaller particles, actual gene release into the cytosol may well be higher, due to the prolonged residence time of the complexes in this compartment, thus avoiding rapid lysosomal degradation. Such an explanation is in agreement with reports that several pathogens, including viruses, bacteria and other parasites enter cells via caveolae, thereby escaping degradation in the lysosomal compartment [13], possibly due to deprivation of the proper signals required for fusion with other cellular compartments [47].

Evidently, the actual size of single flask-shape caveolae is too small for accommodating particles as large as 500 nm. In addition, the beads are obviously also devoid of specific ligands present on viral particles or bacteria, which can be bound and processed via caveolae-localized receptors [13]. Moreover, why are the smaller particles excluded from this internalization pathway? Although a clear explanation is lacking, it can be speculated that electrostatic interactions localize the particles to either clathrin or caveolin-coated domains when they surf across the membrane surface. Evidently, following association with caveolae and given their size, recruitment of an internalization machinery is needed to accommodate particles that extend beyond the actual size of a caveolae domain, which appears possible given internalization of bacteria and viruses along this pathway. A preferential internalization of the larger particles may then be related to a more strict dependence of clathrin-mediated internalization on particle size, i.e. displaying an upper limit of around 200 nm and a more rapid kinetics of internalization, the latter rationalizing why significant entry of smaller particles ($\leqslant 200$ nm) is not apparent via a caveolae-mediated pathway. Consistent with this notion, 100 nm particles never co-localized with 500 nm beads in co-incubation experiments (results not shown). Moreover, over a

© 2004 Biochemical Society

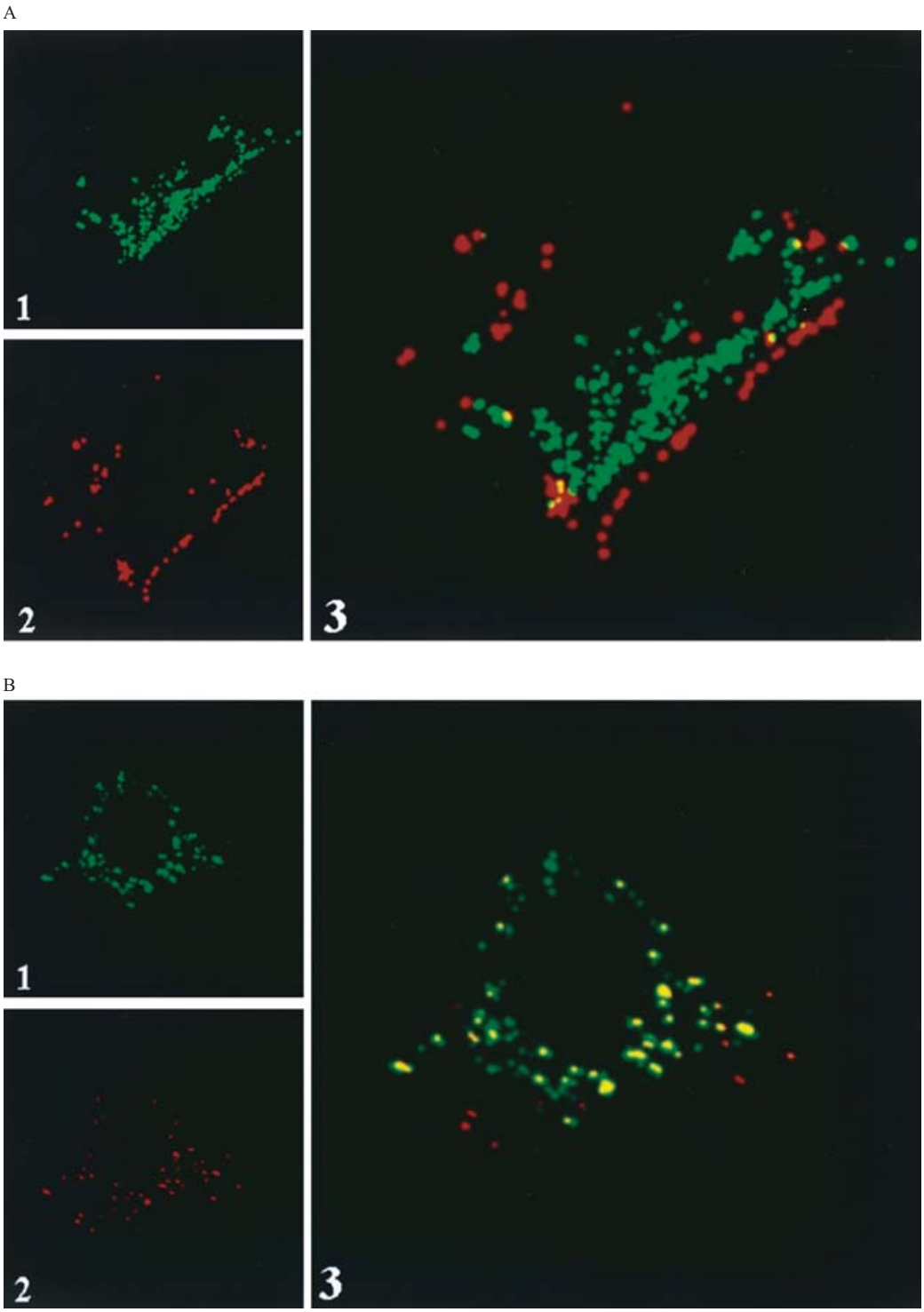

Figure 10 Beads of 200 nm, but not of 500 nm arrive in late endosomal/lysosomal compartments

B16 cells were first incubated with FITC–dextran (green) for 12 h at 37 °C to allow the dye to reach late endosomal/lysosomal compartments. The cells were then incubated with fluorescent 500 (**A**) and 200 (**B**) nm (red) microspheres in serum-free medium for 3 h at 37 °C, which was followed by a 1 h chase. The samples were examined by confocal microscopy (Leica TCS SP2). (**A**) Panel 1, FITC–dextran (green); panel 2, 500 nm beads (red); panel 3, merged picture. (**B**) Panel 1, FITC–dextran (green); panel 2, 200 nm beads (red); panel 3, merged picture.

time period of 30 min, little, if any, uptake of 500 nm beads is seen, whereas, under these conditions, nearly 50 % of the added 50 and 100 nm beads may already have become internalized. Also, given the 200 nm size limit for the clathrin-mediated pathway of internalization, it would then be anticipated that kinetically both processes of internalization may start to compete when the size exceeds this diameter. This is indeed the case.

In conclusion, the present study reveals the relevance of particle size itself, i.e. devoid of ligands, as an important factor in governing the cellular pathway of entry and processing, relevant

© 2004 Biochemical Society

to various recent observations of pathogen entry. In addition, the work may prove useful for the rational design of carriers for drug and gene delivery, the efficiency of which depends on the mode of entry and efficiency of trafficking to the lysosomes. Before reaching this ultimate destination, an early release of the cargo is desirable in order to avoid degradation. Here, a rationale is provided as to why particle size may represent an important parameter in such a programmable mechanism of delivery.

This work was financially supported by a TMR Marie Curie Research Training grant (to J.R.; #ERBFMBICT 51403) and by the Netherlands Foundation for Chemical Research/Netherlands Technology Foundation (CW/STW).

REFERENCES

1 Pedroso de Lima, M. C., Simoes, S., Pires, P., Faneca, H. and Duzgunes, N. (2001) Cationic lipid–DNA complexes in gene delivery: from biophysics to biological applications. Adv. Drug Delivery Rev. **47**, 277–294
2 Zuhorn, I. S. and Hoekstra, D. (2002) On the mechanism of cationic amphiphile-mediated transfection. To fuse or not to fuse: is that the question? J. Membr. Biol. **189**, 167–179
3 Zhang, Y.-P., Reimer, D. L., Zhang, G., Lee, P. H. and Bally, M. B. (1997) Self-assembling DNA–lipid particles for gene transfer. Pharm. Res. **14**, 190–196
4 Wrobel, I. and Collins, D. (1995) Fusion of cationic lipids with mammalian cells occurs after endocytosis. Biochim. Biophys. Acta **1235**, 296–304
5 Zabner, J., Fasbender, A. J., Moninger, T., Poelinger, K. A. and Welsh, M. J. (1995) Cellular and molecular barriers to gene transfer by a cationic lipid. J. Biol. Chem. **270**, 18997–19007
6 Xu, Y. and Szoka, Jr, F. C. (1996) Mechanism of DNA release from cationic liposome/DNA complexes used in cell transfection. Biochemistry **35**, 5616–5623
7 Hafez, I. M., Maurer, N. and Cullis, P. R. (2001) On the mechanism whereby cationic lipids promote intracellular delivery of polynucleic acids. Gene Ther. **8**, 1188–1196
8 Zuhorn, I. S., Visser, W. H., Bakowsky, U., Engberts, J. B. F. N. and Hoekstra, D. (2002) Interference of serum with lipoplex–cell interaction: modulation of intracellular processing. Biochim. Biophys. Acta **1560**, 25–36
9 Zuhorn, I. S., Kalicharan, R. and Hoekstra, D. (2002) Lipoplex-mediated transfection of mammalian cells occurs through the cholesterol-dependent clathrin-mediated pathway of endocytosis. J. Biol. Chem. **277**, 18021–18028
10 Lencer, W. I., Hirst, T. R. and Holmes, R. K. (1999) Membrane traffic and the cellular uptake of cholera toxin. Biochim. Biophys. Acta **1450**, 177–190
11 Stang, E., Kartenbeck, J. and Parton R. G. (1997) Major histocompability complex class I molecules mediate association of SV40 with caveolae. Mol. Biol. Cell **8**, 47–57
12 Anderson, H. A., Chen, Y. and Norkin, L. C. (1998) MHC class I molecules are enriched in caveolae but do not enter with simian virus 40. J. Gen. Virol. **79**, 1469–1477
13 Shin, J.-S. and Abraham, S. N. (2001) Cavaolae as portals of entry for microbes. Microbes Infect. **3**, 755–761
14 Hed, J., Hallden, G., Johanson, S. G. O. and Larsson, P. (1997) The use of fluorescence quenching in flow cytofluorimetry to measure the attachment and ingestion phases in phagocytosis in peripheral blood without prior cell separation. J. Immunol. Methods **101**, 119–125
15 Ohtani, Y., Irie, T., Uekama, K., Fukunaga, K. and Pitha, J. (1989) Differential effects of α-, β- and γ-cyclodextrins on human erythrocytes. Eur. J. Biochem. **186**, 17–22
16 Kilsdonk, E. P., Yancey, P. G., Stoudt, G. W., Bangerter, F. W., Johnson, W. J., Phillips, M. C. and Rothblat, G. H. (1995) Cellular cholesterol efflux mediated by cyclodextrins. J. Biol. Chem. **270**, 17250–17256
17 Rodal, S. K., Skretting, G., Garred, O., Vilhardt, F., van Deurs, B. and Sandvig, K. (1999) Extraction of cholesterol with methyl-β-cyclodextrin perturbs formation of clathrin-coated endocytic vesicles. Mol. Biol. Cell **10**, 961–974
18 Aoki, T., Nomura, R. and Fujimoto, T. (1999) Tyrosine phosphorylation of caveolin-1 in the endothelium. Exp. Cell Res. **253**, 629–636
19 Liu, P. and Anderson, R. G. (1999) Spatial organization of EGF receptor transmodulation by PDGF. Biochem. Biophys. Res. Commun. **261**, 695–700
20 Schnitzer, J. E., Oh, P., Pinney, E. and Allard, J. (1994) Filipin-sensitive caveolae-mediated transport in endothelium: reduced transcytosis, scavenger endocytosis and capillary permeability of select macromolecules. J. Cell Biol. **127**, 1217–1232
21 Orlandi, P. A. and Fishman, P. H. (1998) Filipin-dependent inhibition of cholera toxin: evidence for toxin internalization and activation through caveolae-like domains. J. Cell Biol. **141**, 905–915
22 Wang, L.-H., Rothberg, K. G. and Anderson, R. G. W. (1993) Mis-assembly of clathrin lattices on endosomes reveals a regulatory switch for coated pits formation. J. Cell Biol. **123**, 1107–1117
23 Liu, N. Q., Lossinsky, A. S., Popik, W., Li, X., Gujuluva, C., Kriederman, B., Roberts, J., Pushkarsky, T., Bukrinsky, M., Witte, M. et al. (2002) Human immunodeficiency virus type 1 enters brain microvascular endothelia by macropinocytosis dependent on lipid rafts and the mitogen-activated protein kinase signaling pathway. J. Virol. **76**, 6689–6700
24 Pitha, J., Irie, T., Sklar, P. B. and Nye, J. S. (1988) Drug solubilizers to aid pharmacologists: amphorous cyclodextrin derivatives. Life Sci. **43**, 493–502
25 Grimmer, S., van Deurs, B. and Sandvig, K. (2002) Membrane ruffling and macropinocytosis in A431 cells require cholesterol. J. Cell Sci. **115**, 2953–2962
26 Parton, R. G., Joggerst, B. and Simons, K. (1994) Regulated internalization by caveolae. J. Cell Biol. **127**, 1199–1215
27 Shin, J.-S., Gao, Z. and Abraham, S. N. (2000) Involvement of cellular caveolae in bacterial entry into mast cells. Science **289**, 785–788
28 Rothberg, K. G., Heuser, J. E., Donzel, W. C., Ying, Y.-S., Glenney, J. R. and Anderson, R. G. W. (1992) Caveolin, a protein component of caveolae membrane coat. Cell **68**, 673–682
29 Subtil, A., Gaidarov, I., Kobylarz, K., Lampson, M. A., Keen, J. H. and McGraw, T. E. (1999) Acute cholesterol depletion inhibits clathrin-coated pit budding. Proc. Natl. Acad. Sci. U.S.A. **96**, 6775–6780
30 Larkin, J. M., Brown, M. S., Goldstein, J. L. and Anderson, R. G. W. (1983) Depletion of intracellular potassium arrests coated pit formation and receptor-mediated endocytosis in fibroblasts. Cell **33**, 273–285
31 Benmerah, A., Lamaze, C., Begue, B., Schmid, S., Dautry-Varsat, A. and Cerf-Bensussan, N. (1998) AP-2/Eps15 interaction is required for receptor-mediated endocytosis. J. Cell Biol. **140**, 1055–1062
32 Benmerah, A., Bayrou, M., Cerf-Bensussan, N. and Dautry-Versat, A. (1999) Inhibition of clathrin-coated pit assembly by an Eps15 mutant. J. Cell Sci. **112**, 1303–1311
33 Puri, V., Watanabe, R., Singh, R. D., Dominguez, M., Brown, J. C., Wheatly, C. L., Marks, D. L. and Pagano, R. E. (2001) Clathrin-dependent and -independent internalization of plasma membrane sphingolipids initiates two Golgi targeting pathways. J. Cell Biol. **154**, 535–547
34 Iwabuchi, K., Handa, K. and Hakomori, S. (1998) Separation of "glycosphingolipid signaling domain" from caveolin-containing membrane fraction in mouse melanoma B16 cells and its role in cell adhesion coupled with signaling. J. Biol. Chem. **273**, 33766–33773
35 Dangoria, N. S., Breau, W. C., Anderson, H. A., Cishek, D. M. and Norkin, L. C. (1996) Extracellular simian virus 40 induces an ERK/MAP kinase-independent signaling pathway that activates primary response genes and promotes virus entry. J. Gen. Virol. **777**, 2173–2182
36 Hopwood, D., Spiers, E. M., Ross, P. E., Anderson, J. T., McCullough, J. B. and Murray, F. E. (1995) Endocytosis of fluorescent microspheres by human oesophageal epithelial cells: comparison between normal and inflamed tissue. Gut **37**, 598–602
37 Innes, N. P. T. and Ogden, G. R. (1999) A technique for the study of endocytosis in human oral epithelial cells. Arch. Oral Biol. **44**, 519–523
38 Matlin, K. S., Reggio, H., Helenius, A. and Simons, K. (1982) Pathway of vesicular stomatis virus entry leading to infection. J. Mol. Biol. **156**, 609–631
39 Godbay, W. T., Wu, K. K. and Mikos, A. G. (1999) Tracking the intracellular path of poly(ethylenimine)/DNA complexes for gene delivery. Proc. Natl. Acad. Sci. U.S.A. **96**, 5177–5181
40 Finlay, B. B., Ruschkowski, S. and Dedhar, S. (1991) Cytoskeletal rearrangements accompanying *Salmonella* entry into epithelial cells. J. Cell Sci. **99**, 283–296
41 Ridley, A. J. (1994) Membrane ruffling and signal transduction. BioEssays **16**, 321–327
42 Swanson, J. A. and Watts, C. (1995) Macropinocytosis. Trends Cell Biol. **5**, 424–428
43 Werling, D., Hope, J. C., Chaplin, P., Collins, R. A., Taylor, G. and Howard, C. J. (1999) Involvement of caveolae in the uptake of respiratory syncytial virus antigen by dendritic cells. J. Leukocyte Biol. **66**, 50–58
44 Ross, P. C. and Hui, S. W. (1999) Lipoplex size is a major determinant of *in vitro* lipofection efficiency. Gene Ther. **6**, 651–659
45 Felgner, P. L., Gadek, T. R., Holm, M., Roman, R., Chan, H. W., Wenz, M., Northrop, J. P., Ringold, G. M. and Danielsen, M. (1987) Lipofection: a highly efficient, lipid-mediated DNA-transfection procedure. Proc. Natl. Acad. Sci. U.S.A. **84**, 7413–7417
46 Xu, Y., Hui, S.-W. and Szoka, Jr, F. C. (1999) Physicochemical characterization and purification of cationic lipoplex. Biophys. J. **777**, 341–353
47 Joiner, K. A., Fuhrman, S. A., Miettinen, H. M., Kasper, L. H. and Mellman, I. (1990) *Toxoplasma gondii*: fusion competence of parasitophorous vacuoles in Fc receptor-transfected fibroblasts. Science **249**, 641–664

Received 15 August 2003/24 September 2003; accepted 24 September 2003
Published as BJ Immediate Publication 24 September 2003, DOI 10.1042/BJ20031253

© 2004 Biochemical Society